Regular Form Based Sliding Mode Control Design on a Two-wheeled Inverted Pendulum

Yankun Yang*, Xinggang Yan, Konstantinos Sirlantzis and Gareth Howells

School of Engineering and Digital Arts,
University of Kent, Canterbury, Kent, U.K., CT2 7NZ
E-mail: yy237@kent.ac.uk
E-mail: x.yan@kent.ac.uk
E-mail: k.sirlantzis@kent.ac.uk
E-mail: w.g.j.howells@kent.ac.uk
*Corresponding author

Abstract: In this paper, a Lagrangian-based dynamics is employed for a Two-wheeled Inverted Pendulum with the consideration of unknown matched and unmatched uncertainties which are bounded by known nonlinear functions. The model is linearised and further transformed into a regular form to facilitate the analysis and design. A sliding surface is designed, and a set of conditions is developed such that the resulting sliding motion is uniformly ultimately bounded from a practical perspective. Further, a sliding mode control scheme is proposed such that the system is driven to the sliding surface in finite time and maintained on it thereafter. Finally, both simulation and experiment are presented using practical model parameters data to demonstrate the effectiveness and robustness of the regulation control.

Keywords: Sliding Mode Control, Regular Form, Wheeled Inverted Pendulum, Nonlinear System, Mobile Robots.

Biographical notes: Yankun Yang received the B.Maths degree in Computer Science in 2010 from the University of Waterloo, Ontario, Canada, and the M.Sc. degree (with distinction) in Embedded Systems and Instrumentation in 2016 from the University of Kent, Canterbury, U.K., where he is currently working toward the Ph.D. degree in Electronic Engineering. He has also worked at the Research and Development department in industries for many years mainly in charge with ARM Linux drivers and Apps development under ARM Cortex-A series Android platforms and STM32 ARM Cortex-M related real-time operating system applications. His current research interests include sliding mode control, nonlinear control systems, mobile robot applications.

Xing-Gang Yan received the B.Sc. Degree from Shaanxi Normal University, in 1985, the M.Sc. Degree from Qufu Normal University in 1991, and the Ph.D. Degree of Engineering from Northeastern University, China in 1997. Currently, he is senior lecturer of Control Engineering at the University of Kent, United Kingdom. He worked as a Research Fellow/Research Associate in the University of Hong Kong, China, Nanyang Technological University, Singapore and the University of Leicester, United Kingdom. He is an IEEE member, IET member, HEA Fellow and a Charted Engineer. He has published over 180 referred papers in the area of control engineering. He serves as an Associate Editor of several engineering journals including IET Control Theory and Applications, Energies, and Mathematical Problems in Engineering. His research interests include sliding mode control, decentralised control, fault detection and isolation, and time delay system with applications in engineering systems.

Konstantinos Sirlantzis is currently a Lecturer in image processing and vision with the School of Engineering and Digital Arts, University of Kent, and also a Senior Lecturer in intelligent systems. He has a strong track record in image analysis and understanding, artificial intelligence, and neural networks for pattern recognition and biometrics-based security applications. He currently leads a Research Team working on social assistive and autonomous robotics and healthrelated assistive technologies. He has authored over 100 peer-reviewed articles in journals and conferences.

Gareth Howells is currently a Professor of secure electronic systems. He has been involved in research relating to security, biometrics, and pattern classification techniques for over 25 years. His recent work has been directed toward the development of secure device authentication systems with a focus on the Internet of Things (IoT). He has authored over 180 papers in the technical literature and his recent work has been directed toward the development of secure device authentication systems which has received significant funding from several funding bodies and is currently in the process of being commercially exploited.

1 Introduction

Wheeled mobile robot, particularly Two-wheeled Inverted Pendulum (TWIP), has received great attention to the researchers in recent decades (Kim & Kwon (2017), Yue et al. (2018), Lam & Fujimoto (2019), Sun et al. (2020), Tian et al. (2020), Liu et al. (2020) and Elyoussef et al. (2020)). TWIP is an inherently nonlinear, coupled underactuated system in the sense that the numbers of actuators are less than the degrees of freedom (DOF) to be controlled, which is mentioned in Chan et al. (2013). Conventionally, a TWIP is composed of a body of inverted pendulum and two independently driven wheels attached on the same axle in parallel. The control objective is to maintain the motion of the TWIP whilst balancing the attitude of the pendulum to its equilibrium point at all time.

Many controllers have been proposed for wheeled inverted pendulum in the past, which is summarised by Romlay et al. (2019). Lin & Tsai (2009) applied traditional PID controllers to a human transportation vehicle for teaching purposes. Huang & Yeh (2020) proposed four linear full-state feedback controllers with linear matrix inequalities (LMI) to balance the wheeled mobile vehicles even under the changes of traction environment. However, only the unmatched uncertainties are considered in the system. Pathak et al. (2005) derived partial feedback linearisation equations for designing double two-level velocity balancing and position controllers of a TWIP. Nevertheless, the system dynamics does not consider matched and unmatched uncertainties which might affect the system performance due to the lack of handling uncertainties in controller design. Huang et al. (2018) presented three integrating interval type-2 fuzzy logic controllers to balance and regulate the position and direction of the TWIP. However, the control law does not deal with uncertainties either because of the absence of uncertainty considerations in their system dynamics. Moreover, the use of fuzzy logic method requires sophisticated fuzzy rules to design corresponding controllers, which might not be readily to obtain and the fuzzy logic rule tables also increase the complexity of implementations.

Practical systems often inevitably suffer from uncertainties and disturbances which may affect the system performance tremendously. In Yan et al. (2017), sliding mode control (SMC) has been widely recognised as one of the most popular nonlinear control strategies because of its strong robustness against uncertainty and insensitivity to the parameter variations during the sliding motion. Although matched uncertainties are completely nullified when sliding mode occurs, the reaching phase can still be affected by the matched and unmatched uncertainties which might not be readily reduced or rejected by the control and such uncertainties could affect system performance or even devastate system stability. Numerous SMC techniques have been developed to make classes of linear and nonlinear systems robust enough against disturbances and uncertainties. Edwards & Spurgeon (1998) proposed a regular form based unit vector state feedback algorithm to improve the robustness of the control with the consideration of linear bounds on the matched and unmatched uncertainties. However, the uncertainties and disturbances exerted on practical systems may have nonlinear bounds, which might not be applicable with the method in Edwards & Spurgeon (1998). Yan et al. (2007) proposed an output feedback robust control scheme in the presence of nonlinear disturbances, which mainly focused on unmatched uncertainties with nonlinear bounds. In Yan et al. (2009), a static output feedback control is developed for a class of linear systems to deal with both matched and unmatched uncertainties with unknown structure and nonlinear bounds.

For the applications of TWIP, some of the researchers, nowadays, tend to lump all the disturbances and/or uncertainties together and use disturbance observers to handle them. Huang et al. (2020) proposed a high-order disturbance-observer-based SMC for a practical TWIP. Nevertheless, it is required that the bounds on the lumped uncertainties are linear due to the limitation of the utilisation of LMI technique. In Chen (2017), a nonlinear disturbance observer based SMC is developed with linear bounds on disturbances as well. It should be mentioned that to augment a disturbance observer through the controller design will increase the dimension of the system, which leads to complex implementations. In this paper, the nonlinear system of the TWIP is described based on the Lagrangian dynamics with the consideration of both matched and unmatched uncertainties with nonlinear bounds. Then the system is further linearised and transformed into a regular form. Next, a sliding surface is designed and a SMC strategy is proposed based on the linearised model and the sliding function. The validity and robustness of the control are verified under simulation and experiment on a practical TWIP. Lastly, both results demonstrate that the control scheme is able to balance the TWIP effectively and the system is uniformly ultimately bounded. The main contribution is summarised as follows:

- The bounds on both the matched and the unmatched uncertainties are considered to be known functions, which are employed in the SMC design to reject the uncertainties and enhance the robustness.
- The developed results allow the bounds on the uncertainties to have more general nonlinear form. Thus the results obtained in this paper are able to tolerate a wider class of uncertainties.
- The proposed control is verified on a practical TWIP platform and the experimental results are consistent with the simulation ones.

The remainder of this paper is organised as follows. The system description and control objective of the

TWIP are described in Section 2. The SMC control scheme is designed and the reachability of sliding manifolds along with the stability of the reduced-order sliding motion are analysed in Section 3. Section 4 presents the simulation and experimental results to demonstrate the validity and performance of the proposed control law. Lastly, some conclusions are drawn in Section 5.

2 Problem Formulation

2.1 System Description

This paper only considers the longitudinal motion analysis of the TWIP, which is illustrated in Figure. 1.

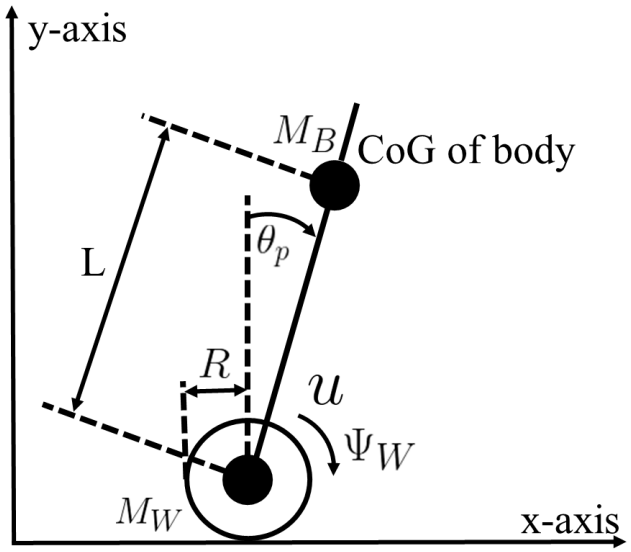

Figure 1: A two-wheeled inverted pendulum

The dynamics of the system is described as follows [See Pathak et al. (2005)].

$$\begin{cases} n_1\ddot{\theta}_p + n_2 cos\theta_p \ddot{\Psi}_W - n_3 sin\theta_p = -u - \tau_B \\ n_4\ddot{\Psi}_W + n_2 cos\theta_p \ddot{\theta}_p - n_2 sin\theta_p \dot{\theta}_p^2 = u + \tau_B - \tau_W \end{cases} \quad (1)$$

where n_i for $i = 1, 2, 3, 4$ are constants and defined by

$$\begin{cases} n_1 = M_B L^2 + J_{\theta_p},\ n_2 = 2M_B LR,\ n_3 = M_B gL \\ n_4 = 4(M_B + M_W)R^2 + J_w \end{cases} \quad (2)$$

θ_p is the attitude pitch angle of the TWIP body, L is the length between the wheel axis and the centre of gravity (CoG) of the body, R is the radius of the wheel, Ψ_W is the angular displacement of the wheel, M_B, M_W are the masses of the TWIP body and wheel respectively, J_{θ_p} is the moment of inertia of the body w.r.t y-axis, and J_w is the moment of inertia of the wheel. Moreover, τ_B, τ_W are the friction torque forces related to the TWIP body and the ground, u represents the total torque (control input) applied to the wheels.

The nonlinear system (1) can be further rewritten as

$$\dot{x}(t) = \mathcal{F}(x(t)) + \mathcal{G}(x(t))(u(t) + f_m(t,x)) + f_{u_1}(t,x) \quad (3)$$

where

$$\mathcal{F}(x) = \begin{bmatrix} x_2 \\ -\frac{n_2 n_3 cosx_3 sinx_3}{n_1 n_4 - n_2^2 cos^2(x_3)} + \frac{n_1 n_2 sinx_3}{n_1 n_4 - n_2^2 cos^2(x_3)} x_4^2 \\ x_4 \\ \frac{n_3 n_4 sinx_3}{n_1 n_4 - n_2^2 cos^2(x_3)} - \frac{n_2^2 sinx_3 cosx_3}{n_1 n_4 - n_2^2 cos^2(x_3)} x_4^2 \end{bmatrix}$$

$$\mathcal{G}(x) = \begin{bmatrix} 0 \\ \frac{n_1 + n_2 cosx_3}{n_1 n_4 - n_2^2 cos^2(x_3)} \\ 0 \\ -\frac{n_2 cosx_3 + n_4}{n_1 n_4 - n_2^2 cos^2(x_3)} \end{bmatrix},\ f_m = \tau_B \quad (4)$$

$$f_{u_1} = \begin{bmatrix} 0 \\ -\frac{n_1}{n_1 n_4 - n_2^2 cos^2(x_3)} \\ 0 \\ \frac{n_2 cosx_3}{n_1 n_4 - n_2^2 cos^2(x_3)} \end{bmatrix} \tau_W$$

$x(t) = [x_1, x_2, x_3, x_4]^T = [\Psi_W, \dot{\Psi}_W, \theta_p, \dot{\theta}_p]^T$ is defined as the state vector, f_m represents the internal joint friction which can be treated as the input channel of the control signal and categorised to the unknown matched uncertainty. f_{u_1} is the unknown unmatched uncertainty which is the correlation between the ground and the wheels, such as the lateral slippage of the robot.

2.2 Preliminaries

For given desired signals $x_d(t) = [x_{1_d}, x_{2_d}, x_{3_d}, x_{4_d}]^T$. The problem considered in this paper is to design a SMC controller such that the system (3) is able to track the desired signals, that is

$$\lim_{t\to\infty} \left| x_i(t) - x_{i_d}(t) \right| = 0 \quad for\ i = 1, 2, 3, 4 \quad (5)$$

For simplification purpose, system (3) can be linearised around the desired signals $x_d(t)$ as

$$\dot{x}(t) = \mathcal{A}x(t) + \mathcal{B}(u(t) + f_m(t,x)) + f_{u_2}(t,x) \quad (6)$$

where $\mathcal{A}$ and $\mathcal{B}$ are constant matrices defined by

$$\mathcal{A} = \left.\frac{\partial \mathcal{F}(x)}{\partial x}\right|_{x=x_d} = \begin{bmatrix} 0 & 1 & 0 & 0 \\ 0 & 0 & \frac{-n_2 n_3}{n_1 n_4 - n_2^2} & 0 \\ 0 & 0 & 0 & 1 \\ 0 & 0 & \frac{n_3 n_4}{n_1 n_4 - n_2^2} & 0 \end{bmatrix}$$

$$\mathcal{B} = \left.\frac{\partial \mathcal{G}(x)}{\partial u}\right|_{x=x_d} = \begin{bmatrix} 0 \\ \frac{n_1 + n_2}{n_1 n_4 - n_2^2} \\ 0 \\ -\frac{n_2 + n_4}{n_1 n_4 - n_2^2} \end{bmatrix} \quad (7)$$

f_m is defined in (4) and f_{u_2} is given by

$$f_{u_2} = \begin{bmatrix} 0 \\ -\frac{n_1}{n_1 n_4 - n_2^2} \\ 0 \\ \frac{n_2}{n_1 n_4 - n_2^2} \end{bmatrix} \tau_W \quad (8)$$

Further, the following assumptions are imposed on system (6).

Assumption 1: The matrix pair $(\mathcal{A}, \mathcal{B})$ is controllable.

Assumption 2: There exist known continuous nonlinear functions $\beta(t,x)$ and $\gamma(t,x)$ such that the unknown matched and unmatched uncertainties $f_m(t,x)$, $f_{u_2}(t,x)$ are bounded and satisfy [See Yan et al. (2007)]

$$\begin{aligned} \left\|f_m(t,x)\right\| &\leq \beta(t,x) \\ \left\|f_{u_2}(t,x)\right\| &\leq \gamma(t,x) \end{aligned} \tag{9}$$

Remark 1: In this paper, the upper bounds of $\left\|f_m(t,x)\right\|$ and $\left\|f_{u_2}(t,x)\right\|$ in Assumption 2 are required to be known functions, which will be employed in the control design to reduce or reject the system uncertainties.

According to the objective from (5), define the error states to be $e = [e_1, e_2, e_3, e_4]^T = [x_1 - x_{1_d}, x_2 - x_{2_d}, x_3 - x_{3_d}, x_4 - x_{4_d}]^T$ and error dynamics of the longitudinal system based on (6) can be described as

$$\dot{e}(t) = \mathcal{A}e(t) + \mathcal{B}(u(t) + f_m(t, e + x_d)) + f_{u_3}(t, e + x_d) \tag{10}$$

where f_m, $\mathcal{A}$, $\mathcal{B}$ are defined in (4) and (7), the unmatched uncertainty $f_{u_3}(t, e + x_d) = f_{u_2}(t, e + x_d) + \mathcal{A}x_d - \dot{x}_d$.

From Assumption 2, $f_m(t, e + x_d)$ and $f_{u_3}(t, e + x_d)$ satisfy

$$\begin{aligned} \left\|f_m(t, e + x_d)\right\| &\leq \beta(t, e + x_d) \\ \left\|f_{u_3}(t, e + x_d)\right\| &\leq \gamma\big(t, e + x_d\big) + \left\|\mathcal{A}\right\|\left\|x_d\right\| + \left\|\dot{x}_d\right\| \end{aligned} \tag{11}$$

3 Sliding Mode Analysis and Control Design

Since the error dynamics (10) is not constructed in a well-known regular form, which is not readily apparent for stability analysis of SMC, introduce a new coordinate transformation.

$$\omega(t) = [\omega_1, \omega_2, \omega_3, \omega_4]^T = T_r e(t) \tag{12}$$

$$T_r = \begin{bmatrix} 1 & 0 & 0 & 0 \\ 0 & 1 & 0 & \Theta \\ 0 & 0 & 1 & 0 \\ 0 & 0 & 0 & 1 \end{bmatrix} \tag{13}$$

where $\Theta = \frac{n_1+n_2}{n_2+n_4}$, and it is clear that T_r is non-singular.

Hence, system (10) can be described in regular form in terms of the new coordinates $\omega(t)$ as

$$\dot{\omega}(t) = \bar{\mathcal{A}}\omega(t) + \bar{\mathcal{B}}\big(u(t) + f_m(t,\omega)\big) + f_{u_4}(t,\omega) \tag{14}$$

where

$$\begin{aligned} \bar{\mathcal{A}} &= \begin{bmatrix} 0 & 1 & 0 & -\Theta \\ 0 & 0 & \frac{n_3}{n_2+n_4} & 0 \\ 0 & 0 & 0 & 1 \\ 0 & 0 & \frac{n_3 n_4}{n_1 n_4 - n_2^2} & 0 \end{bmatrix} \\ \bar{\mathcal{B}} &= \begin{bmatrix} 0 \\ \mathcal{B}_2 \end{bmatrix} = \begin{bmatrix} 0 \\ 0 \\ 0 \\ -\frac{n_2+n_4}{n_1 n_4 - n_2^2} \end{bmatrix} \end{aligned} \tag{15}$$

$f_m(t,\omega)$ and $f_{u_4}(t,\omega)$ are the matched and unmatched uncertainties in ω-system.

The following assumption is imposed on system (14).

Assumption 3: The term $\mathcal{B}_2$ is non-zero.

Based on Assumption 2 and (11), (12),

$$\begin{aligned} \left\|f_m(t,\omega)\right\| &\leq \beta(t, T_r^{-1}\omega + x_d) \\ \left\|f_{u_4}(t,\omega)\right\| &\leq \gamma(t, T_r^{-1}\omega + x_d) + \left\|\mathcal{A}\right\|\left\|x_d\right\| + \left\|\dot{x}_d\right\| \end{aligned} \tag{16}$$

For further analysis, partition $f_{u_4}(t,\omega)$ into

$$f_{u_4}(t,\omega) = \begin{bmatrix} 0 \\ f_{u_{41}}(t,\omega) \\ \hline 0 \\ f_{u_{42}}(t,\omega) \end{bmatrix} \tag{17}$$

Consider the switching function

$$\sigma(t) = \delta_1\omega_1(t) + \delta_2\omega_2(t) + \delta_3\omega_3(t) + \omega_4(t) \tag{18}$$

where δ_1, δ_2, δ_3 are design parameters.

Then, the sliding surface is described by

$$\sigma(t) = \delta_1\omega_1(t) + \delta_2\omega_2(t) + \delta_3\omega_3(t) + \omega_4(t) = 0 \tag{19}$$

Hence, when sliding motion occurs, $\omega_4(t)$ can be expressed in terms of $\omega_1(t)$, $\omega_2(t)$, and $\omega_3(t)$ as

$$\omega_4(t) = -\delta_1\omega_1(t) - \delta_2\omega_2(t) - \delta_3\omega_3(t) \tag{20}$$

3.1 Stability Analysis of Sliding Motion

From (14), (15), and (20), it is straightforward to see that the reduced-order sliding mode system when confined to the sliding surface $\sigma(t) = 0$ can be derived as

$$\dot{\omega}_s(t) = \underbrace{\begin{bmatrix} \Theta\delta_1 & \Theta\delta_2 + 1 & \Theta\delta_3 \\ 0 & 0 & \frac{n_3}{n_2+n_4} \\ -\delta_1 & -\delta_2 & -\delta_3 \end{bmatrix}}_{\widetilde{\mathcal{A}}_{11}^s} \omega_s(t) + \underbrace{\begin{bmatrix} 0 \\ f_{u_{41}} \\ 0 \end{bmatrix}}_{\widetilde{f}_{u_{41}}} \tag{21}$$

where $\omega_s(t) = [\omega_1(t), \omega_2(t), \omega_3(t)]^T$.

The following assumption is imposed on system (21).

Assumption 4: $\frac{n_3}{n_2+n_4}$ is a non-zero constant.

Lemma 1: *Consider the reduced-order sliding mode dynamics (21), and suppose Assumptions 1,2 and 4 are satisfied, $\widetilde{\mathcal{A}}_{11}^s$ is Hurwitz stable if the following inequalities hold for δ_1, δ_2 and δ_3.*

$$\delta_1 > 0,\ \delta_2 > \frac{\delta_1}{\delta_3 - \Theta\delta_1},\ \delta_3 > \Theta\delta_1 \tag{22}$$

Proof. The characteristic equation of $\widetilde{\mathcal{A}}_{11}^s$ can be described by

$$z^3 + \big(\delta_3 - \Theta\delta_1\big)z^2 + \frac{n_3}{n_2+n_4}\delta_2 z + \frac{n_3}{n_2+n_4}\delta_1 = 0 \tag{23}$$

The corresponding coefficients of the first column of the Routh-hurwitz array are determined as

$$\begin{aligned} &a_0 = 1,\ a_1 = \delta_3 - \Theta\delta_1 \\ &b_1 = \frac{\frac{n_3\delta_2}{n_2+n_4}\big(\delta_3 - \Theta\delta_1\big) - \frac{n_3}{n_2+n_4}\delta_1}{\delta_3 - \Theta\delta_1} \\ &c_1 = \frac{n_3}{n_2+n_4}\delta_1 \end{aligned} \tag{24}$$

By direct calculation, it follows that a_0, a_1, b_1 and c_1 in (24) are positive if the inequalities in (22) hold. Then under Assumption 4 and based on the Routh-Hurwitz stability criterion, the matrix $\widetilde{\mathcal{A}}_{11}^s$ is stable. ■

From Lemma 1, if δ_1, δ_2 and δ_3 satisfy (22), $\widetilde{\mathcal{A}}_{11}^s$ is stable, which implies that for any symmetric positive definite matrix $Q \in \mathbb{R}^{3\times3}$, there exists a unique symmetric positive definite matrix $P \in \mathbb{R}^{3\times3}$ satisfying the Lyapunov equation

$$\widetilde{\mathcal{A}}_{11}^{s^T} P + P\widetilde{\mathcal{A}}_{11}^s = -Q \tag{25}$$

Theorem 1: *Under the conditions of Lemma 1, the state $\omega_s(t)$ of the sliding mode dynamics (21) is uniformly ultimately bounded.*

Proof. For system (21), consider the candidate Lyapunov function

$$V(\omega_s) = \omega_s^T P \omega_s$$

Then, the time derivative of V along the trajectories of sliding mode dynamics (21) is given by

$$\begin{aligned} \dot{V} &= -\omega_s^T Q\omega_s + 2\omega_s^T P\widetilde{f}_{u_{41}}(t,\omega) \\ &\le -\omega_s^T Q\omega_s + 2\big\|P\omega_s\big\|\big\|\widetilde{f}_{u_{41}}(t,\omega)\big\| \\ &\le -\lambda_{min}(Q)\big\|\omega_s\big\|^2 + 2\lambda_{max}(P)\big\|\omega_s\big\|\big\|\widetilde{f}_{u_{41}}(t,\omega)\big\| \\ &\le -\lambda_{max}(P)\big\|\omega_s\big\|\bigg(\frac{\lambda_{min}(Q)}{\lambda_{max}(P)}\big\|\omega_s\big\| - 2\Big(\gamma(t,T_r^{-1}\omega + x_d) \\ &\quad + \big\|\mathcal{A}\big\|\big\|x_d\big\| + \big\|\dot{x}_d\big\|\Big)\bigg) \end{aligned} \tag{26}$$

where the condition (16) is used above. In addition, $\lambda_{min}(\cdot)$, $\lambda_{max}(\cdot)$ denote the minimum and maximum eigenvalues of the corresponding matrices respectively.

Consequently, $\dot{V} \le 0$ if

$$\big\|\omega_s\big\| \ge \frac{2\Big(\gamma(t,T_r^{-1}\omega + x_d) + \big\|\mathcal{A}\big\|\big\|x_d\big\| + \big\|\dot{x}_d\big\|\Big)}{\lambda_{min}(Q)/\lambda_{max}(P)}$$

Hence, the conclusion follows. ■

Remark 2: It is obvious to notice from (21) that the sliding motion is only affected by the unmatched uncertainty $\widetilde{f}_{u_{41}}(t,\omega)$, which is consistent with the conclusion [See Yan et al. (2017)] that the reduced sliding mode dynamics is insensitive to matched uncertainty.

3.2 Sliding Mode Control Design

The objective of this section is to design a controller such that the reachability condition [see Yan et al. (2017)]

$$\sigma^T(t)\dot{\sigma}(t) \le -\rho\big\|\sigma(t)\big\| \tag{27}$$

is satisfied for some positive constant ρ, where $\sigma(t)$ is the switching function defined in (18).

The following SMC law is proposed

$$\begin{aligned} u(t) = -\mathcal{B}_2^{-1}\Bigg\{&\delta_1\omega_2 + \bigg(\frac{n_3n_4}{n_1n_4 - n_2^2} + \frac{n_3}{n_2+n_4}\delta_2\bigg)\omega_3 \\ &+ (\delta_3 - \Theta\delta_1)\omega_4 + \Bigg[\big|\mathcal{B}_2\big|\beta(t,T_r^{-1}\omega + x_d) \\ &+ \Big(\big|\delta_2\big| + 1\Big)\Big(\gamma(t,T_r^{-1}\omega + x_d) + \big\|\mathcal{A}\big\|\big\|x_d\big\| + \big\|\dot{x}_d\big\|\Big) \\ &+ \rho\Bigg]\frac{\sigma(t)}{\big\|\sigma(t)\big\|}\Bigg\} \end{aligned} \tag{28}$$

where $\beta(\cdot)$ and $\gamma(\cdot)$ are given in (16).

Theorem 2: *Consider the system in (14), the control (28) is able to drive system (14) to the sliding surface (19) in finite time and maintain a sliding motion on it thereafter.*

Proof. From the definition of $\sigma(t)$ in (18), it follows that

$$\begin{aligned} \dot{\sigma}(t) = &\delta_1\omega_2 + \bigg(\frac{n_3n_4}{n_1n_4 - n_2^2} + \frac{n_3}{n_2+n_4}\delta_2\bigg)\omega_3 \\ &+ (\delta_3 - \Theta\delta_1)\omega_4 + \mathcal{B}_2\Big(u(t) + f_m(t,\omega)\Big) \\ &+ \delta_2 f_{u_{41}}(t,\omega) + f_{u_{42}}(t,\omega) \end{aligned} \tag{29}$$

Substituting the designed control law (28) into (29) yields

$$\begin{aligned} \dot{\sigma}(t) = -\Bigg[&\big|\mathcal{B}_2\big|\beta(t,T_r^{-1}\omega + x_d) + \Big(\big|\delta_2\big| + 1\Big) \\ &\times \Big(\gamma(t,T_r^{-1}\omega + x_d) + \big\|\mathcal{A}\big\|\big\|x_d\big\| + \big\|\dot{x}_d\big\|\Big) + \rho\Bigg] \\ &\times \frac{\sigma(t)}{\big\|\sigma(t)\big\|} + \mathcal{B}_2 f_m(t,\omega) + \delta_2 f_{u_{41}}(t,\omega) + f_{u_{42}}(t,\omega) \end{aligned} \tag{30}$$

Therefore,

$$\begin{aligned}\sigma^T(t)\dot{\sigma}(t) \leq & -\|\sigma\|\Bigg\{\Bigg[|\mathcal{B}_2|\beta(t,T_r^{-1}\omega+x_d)+\Big(|\delta_2|+1\Big)\\ & \times\Big(\gamma(t,T_r^{-1}\omega+x_d)+\|\mathcal{A}\|\|x_d\|+\|\dot{x}_d\|\Big)+\rho\Bigg]\\ & -|\mathcal{B}_2|\|f_m(t,\omega)\|-|\delta_2|\|f_{u_{41}}(t,\omega)\|\\ & -\|f_{u_{42}}(t,\omega)\|\Bigg\}\\ \leq & -\|\sigma\|\Bigg\{\Bigg[|\mathcal{B}_2|\beta(t,T_r^{-1}\omega+x_d)+\Big(|\delta_2|+1\Big)\\ & \times\Big(\gamma(t,T_r^{-1}\omega+x_d)+\|\mathcal{A}\|\|x_d\|+\|\dot{x}_d\|\Big)+\rho\Bigg]\\ & -|\mathcal{B}_2|\beta(t,T_r^{-1}\omega+x_d)-|\delta_2|\Big(\gamma(t,T_r^{-1}\omega+x_d)\\ & +\|\mathcal{A}\|\|x_d\|+\|\dot{x}_d\|\Big)-\Big(\gamma(t,T_r^{-1}\omega+x_d)\\ & +\|\mathcal{A}\|\|x_d\|+\|\dot{x}_d\|\Big)\Bigg\}\\ \leq & -\rho\|\sigma(t)\| \end{aligned} \tag{31}$$

where ρ is defined in (27). Inequality (31) shows that the reaching condition (27) is satisfied. Hence the result follows. ■

Remark 3: Based on SMC theory, Theorem 1 and 2 together show that the closed-loop system formed by applying the control (28) to the system (14) is uniformly ultimately bounded. From (12), it follows that

$$e(t) = T_r^{-1}\omega(t) \tag{32}$$

where T_r is defined in (13).
Therefore, the tracking error $e(t)$ is also uniformly ultimately bounded.

4 Simulation and Experiment Research

The verification of the proposed control law is conducted under both simulation and experiment, which will be elaborated in this section.

4.1 Numerical Simulation

The simulation is tested under the scenario with which the TWIP is driven on a flat surface. The control aim is to balance the TWIP to the desired equilibrium $x_d = [0,0,0,0]^T$. By using the data from Table 1, the corresponding system can be described based on (6), (7) and (8) as

Table 1 Model parameters for the TWIP

Symbols with units	Definitions	Values
M_B [kg]	Mass of body	1.008
M_W [kg]	Mass of wheel	0.179
R [m]	Radius of wheel	0.06
L [m]	Length to CoG	0.09
J_W [kg.m^2]	Inertial of wheel	0.00032
J_{P_θ} [kg.m^2]	y-axis inertial of body	0.0027

$$\begin{aligned}\dot{x}(t) = & \underbrace{\begin{bmatrix}0 & 1 & 0 & 0\\ 0 & 0 & -137.0893 & 0\\ 0 & 0 & 0 & 1\\ 0 & 0 & 219.2744 & 0\end{bmatrix}}_{\mathcal{A}} x(t)\\ & + \underbrace{\begin{bmatrix}0\\ 307.7729\\ 0\\ -400.4251\end{bmatrix}}_{\mathcal{B}} (u(t)+f_m(t,x)) + \underbrace{\begin{bmatrix}0\\ -153.7336\\ 0\\ 154.0393\end{bmatrix}}_{f_{u_2}(t,x)} \tau_W \end{aligned} \tag{33}$$

It can be verified that the matrix pair $(\mathcal{A},\mathcal{B})$ is controllable. Therefore, Assumption 1 is satisfied.

Based on Assumption 2 and system (33), the unknown signals $f_m(t,x)$ and $f_{u_2}(t,x)$, defined in (4) and (8), satisfy

$$\begin{aligned}\|f_m(t,x)\| = \|\tau_B\| &\leq \underbrace{\frac{1}{40}|x_4| + \frac{7}{200}sin^2(x_4)}_{\beta(t,x)}\\ \|f_{u_2}(t,x)\| &= \left\|\begin{bmatrix}0\\ -153.7336\\ 0\\ 154.0393\end{bmatrix}\right\| \|\tau_W\|\\ &\leq \underbrace{217.6284\left(\frac{11}{200}|x_2| + \frac{6}{125}sin^2(x_2)\right) + 5.0}_{\gamma(t,x)} \end{aligned} \tag{34}$$

Choose $\delta_1 = 6.9$, $\delta_2 = 2.2$ and $\delta_3 = 13.7$ satisfying the conditions (22) of Lemma 1. The corresponding switching function is determined as

$$\sigma(t) = 6.9\omega_1(t) + 2.2\omega_2(t) + 13.7\omega_3(t) + \omega_4(t) \tag{35}$$

Further, based on the system in (14), it follows that the regular form of (33) can be described by

$$\dot{\omega}(t) = \underbrace{\begin{bmatrix} 5.3034 & 2.6910 & 10.53 & 0 \\ 0 & 0 & 31.4484 & 0 \\ -6.9 & -2.2 & -13.7 & 0 \\ 0 & 0 & 219.2744 & 0 \end{bmatrix}}_{\bar{\mathcal{A}}} \omega(t) + \underbrace{\begin{bmatrix} 0 \\ 0 \\ 0 \\ -400.4251 \end{bmatrix}}_{\bar{\mathcal{B}}} \Big(u(t) + f_m(t,\omega)\Big) + \underbrace{\begin{bmatrix} 0 \\ f_{u_{41}}(t,\omega) \\ 0 \\ f_{u_{42}}(t,\omega) \end{bmatrix}}_{f_{u_4}(t,\omega)} \tag{36}$$

It is noticeable from (36) that $\mathcal{B}_2 = -400.4251 \neq 0$. Hence, Assumption 3 is held.

According to the coordinate transformation (12) and the conditions of (11), (16), (34), it follows that $f_m(t,\omega)$ and $f_{u_4}(t,\omega)$ in (36) satisfy

$$\begin{aligned} \big\|f_m(t,\omega)\big\| &\leq \underbrace{\frac{1}{40}\big|\omega_4(t) + x_{4_d}(t)\big| + \frac{7}{200}sin^2(\omega_4(t) + x_{4_d}(t))}_{\beta(t,T_r^{-1}\omega + x_d)} \\ \big\|f_{u_4}(t,\omega)\big\| &\leq \underbrace{\begin{aligned} &217.6284\bigg(\frac{11}{200}\big|\omega_2 - 0.7686\omega_4 + x_{2_d}\big| \\ &\quad + \frac{6}{125}sin^2(\omega_2 - 0.7686\omega_4 + x_{2_d})\bigg) + 5.0 \end{aligned}}_{\gamma(t,T_r^{-1}\omega + x_d)} \end{aligned} \tag{37}$$

From the system matrix $\bar{\mathcal{A}}$ in (36) and the matrix $\widetilde{\mathcal{A}}_{11}^s$ defined in (21), it follows that

$$\widetilde{\mathcal{A}}_{11}^s = \begin{bmatrix} 5.3034 & 2.6910 & 10.53 \\ 0 & 0 & 31.4484 \\ -6.9 & -2.2 & -13.7 \end{bmatrix} \tag{38}$$

It is straightforward to check that $\frac{n_3}{n_2+n_4} = 31.4484 \neq 0$. Hence, Assumption 4 is satisfied, and $\widetilde{\mathcal{A}}_{11}^s$ is Hurwitz stable.

Therefore, for $Q = I_3$, the solution of Lyapunov equation (25) is

$$P = \begin{bmatrix} 2.9859 & 0.4012 & 2.3675 \\ 0.4012 & 0.2210 & 0.7180 \\ 2.3675 & 0.7180 & 3.5043 \end{bmatrix} \tag{39}$$

The designed SMC control law is

$$\begin{aligned} u(t) = 0.0025\Bigg\{ &6.9\omega_2 + 288.4607\omega_3 + 8.3966\omega_4 \\ &+ \Bigg[400.4251\bigg(\frac{1}{40}\big|\omega_4(t) + x_{4_d}(t)\big| + \frac{7}{200}sin^2\big(\omega_4(t) \\ &+ x_{4_d}(t)\big)\bigg) + 3.2\bigg(217.6284\Big(\frac{11}{200}\big|\omega_2(t) + x_{2_d}(t) \\ &- 0.7686\omega_4(t)\big| + \frac{6}{125}sin^2\big(\omega_2(t) - 0.7686\omega_4(t) \\ &+ x_{2_d}(t)\big)\Big) + 5.0\bigg) + \rho\Bigg]\frac{\sigma(t)}{\|\sigma(t)\|}\Bigg\} \end{aligned} \tag{40}$$

For simulation purpose, the initial condition is chosen as $x_0 = [0.02,\ 0,\ 0.4363,\ 0]^T$, which implies that the initial position is 0.02 metre and the initial attitude angle is 0.4363 in radian. Moreover, the control design parameter $\rho = 5.0$. The time responses of the system states and errors are shown in Figure. 2 and Figure. 3 respectively, and the control signal, described in pulse width modulation (PWM) under 12V, is shown in Figure. 4. The results demonstrate the effectiveness and robustness of the controller, which are uniformly ultimately bounded as proved in Theorem 1.

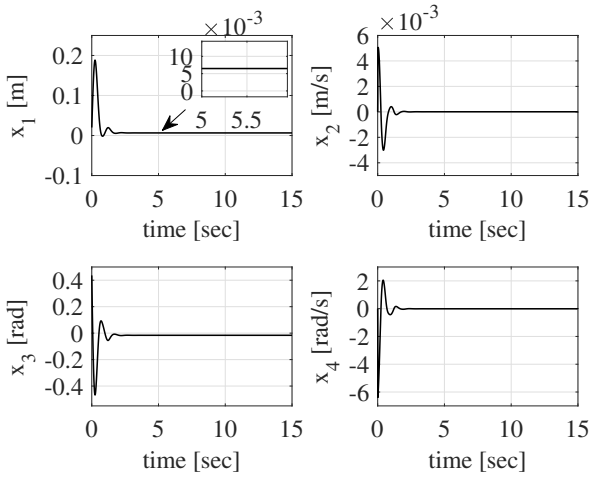

Figure 2: The responses of the system states under simulation

4.2 Experimental Study

In this section, the detailed experiment results will be presented. A prototype TWIP has been fabricated in the laboratory as illustrated in Figure. 5. The dimension of this TWIP is 0.29m width x 0.153m depth x 0.192m height and it weighs for 1.366 kg in total including the body and two wheels. The detailed parameters of the TWIP are given in Table 1. The attitude data are collected using a 9-axis inertia measurement unit (IMU), which are filtered by the Mahony algorithm [See Mahony

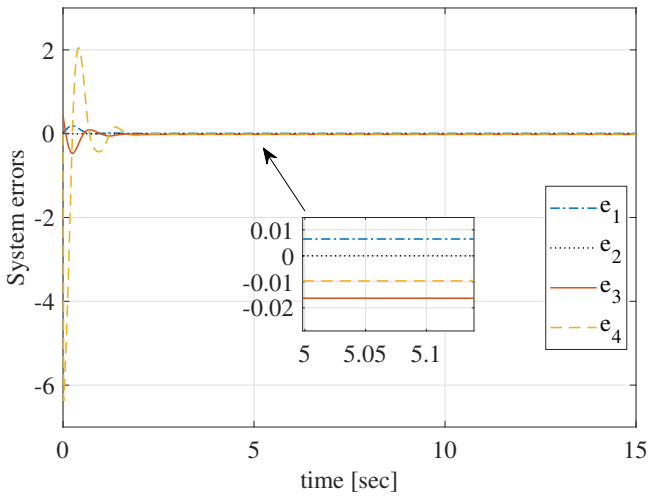

Figure 3: The responses of the error system under simulation

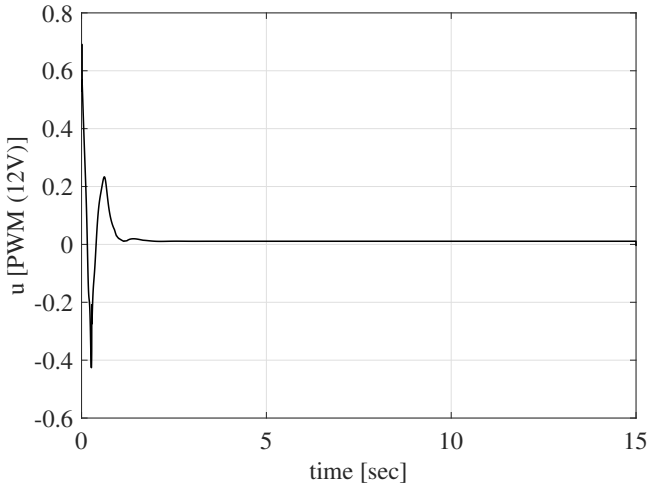

Figure 4: The response of the control under simulation

et al. (2008)] to retrieve the Euler angles. Moreover, two 12V DC motors with 1920 counts per revolution quadrature encoders are attached on the TWIP to control the motion as well as the balance of the TWIP, which are driven by PWM signals generated from an ARM-based STM32F407 microcontroller board.

The experimentation shows that the obtained experiment results are in consistence with the corresponding simulation results. The TWIP is placed stationary on a flat surface and tilted with initial attitude angle $x_3 = 0.4363$ rad and the initial position at $x_1 = 0.02$ metre. Figures. 6 and 7 show the time responses of the system states and errors. Figure. 8 illustrates the control signal to balance the TWIP to the equilibrium status.

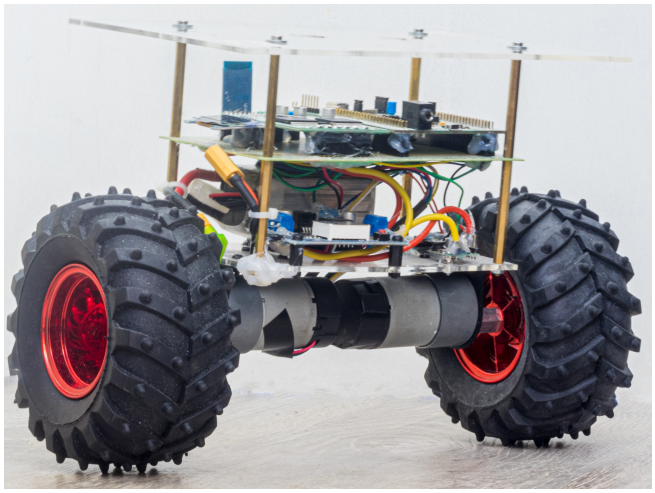

Figure 5: The photograph of the TWIP platform

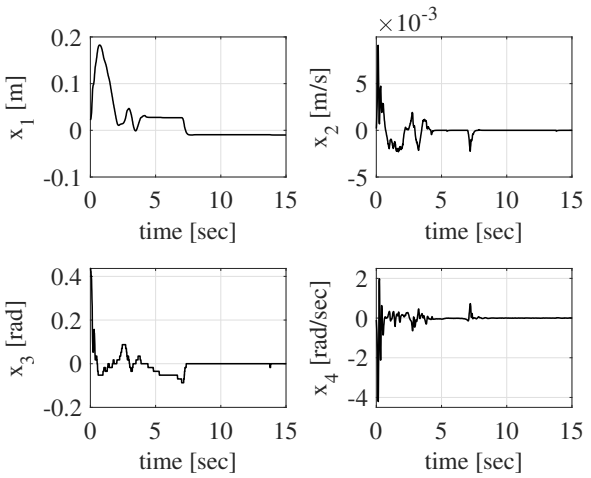

Figure 6: The responses of the system states on a practical TWIP platform

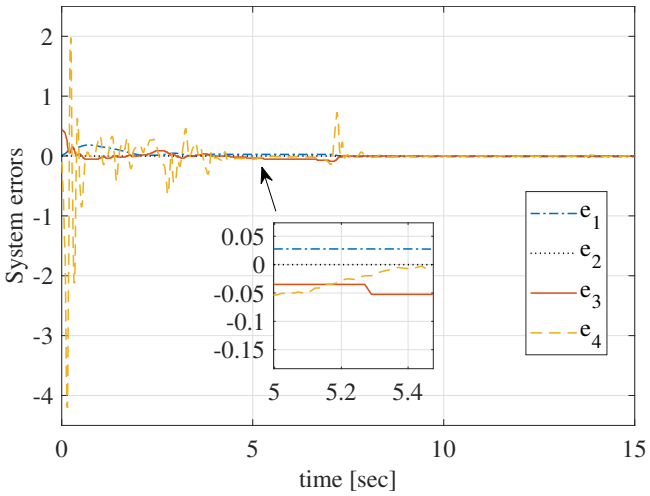

Figure 7: The responses of the error system on a practical TWIP platform

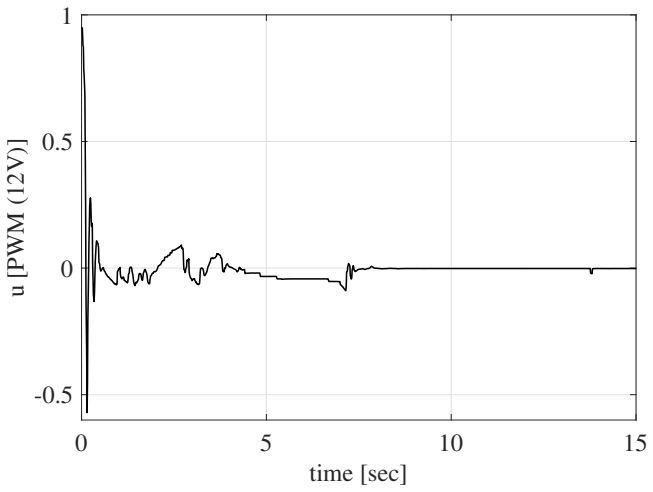

Figure 8: The response of the control on a practical TWIP platform

5 Conclusion

In this paper, a SMC strategy has been proposed for a TWIP system which is experienced matched and unmatched uncertainties. The pre-defined non-linear bounds on the uncertainties are considered and involved in the control design process. The developed results have lower conservatism due to the fact that the utilisation of reduced-order sliding mode dynamics as well as the bounds on uncertainties. It is demonstrated that the system states are uniformly ultimately bounded from both simulation and practical experiment. Finally, the effectiveness and robustness of the control law are not only verified in MATLAB simulation but also on a physical TWIP platform. The future research will focus on the TWIP system driving on an inclined surface, and a novel SMC is to be designed to directly control the nonlinear TWIP system.

Acknowledgement

The research is part financed by European Union ERDF (European Regional Development Fund) through the Interreg IVA "2 Mers Seas Zeeën" cross-border cooperation program (2014-2020) under the project "Empowerment of Disabled people through the User Coproduction of Assistive Technology (EDUCAT)".

References

Chan, R. P. M., Stol, K. A., & Halkyard, C. R. (2013). Review of modelling and control of two-wheeled robots. *Annual Reviews in Control*, *37*, 89–103.

Chen, M. (2017). Robust tracking control for self-balancing mobile robots using disturbance observer. *IEEE/CAA Journal of Automatica Sinica*, *4*(3), 458–465.

Edwards, C. & Spurgeon, S. K. (1998). *Sliding Mode Control: Theory and Applications*. London, U.K: Taylor & Francis.

Elyoussef, E. S., Martins, N. A., Bertol, D. W., Pieri, E. R. D., & Moreno, U. F. (2020). Simulation results and practical implementation of a pd-super-twisting second order sliding mode tracking control for a differential wheeled mobile robot. *International Journal of Computer Applications in Technology*, *63*(3), 213–227.

Huang, C. F. & Yeh, T. J. (2020). Anti slip balancing control for wheeled inverted pendulum vehicles. *IEEE Transactions on Control Systems Technology*, *28*(3), 1042–1049.

Huang, J., Ri, M. H., Wu, D. R., & Ri, S. H. (2018). Interval type-2 fuzzy logic modeling and control of a mobile two-wheeled inverted pendulum. *IEEE Transactions on Fuzzy Systems*, *26*(4), 2030–2038.

Huang, J., Zhang, M. S., Ri, S. H., Xiong, C. H., Li, Z. J., & Kang, Y. (2020). High-order disturbance-observer-based sliding mode control for mobile wheeled inverted pendulum systems. *IEEE Transactions on Industrial Electronics*, *67*(3), 2030–2041.

Kim, S. & Kwon, S. J. (2017). Nonlinear optimal control design for underactuated two-wheeled inverted pendulum mobile platform. *IEEE/ASME Transactions on Mechatronics*, *22*(6), 2803–2808.

Lam, P. V. & Fujimoto, Y. (2019). A robotic cane for balance maintenance assistance. *IEEE Transactions on Industrial Informatics*, *15*(7), 3998 – 4009.

Lin, S. C. & Tsai, C. C. (2009). Development of a self-balancing human transportation vehicle for the teaching of feedback control. *IEEE Transactions on Education*, *52*(1), 157–168.

Liu, Y. Q., Jing, H., Liu, X., & Lv, Y. L. (2020). An improved hybrid error control path tracking intelligent algorithm for omnidirectional agv on ros. *International Journal of Computer Applications in Technology*, *64*(2), 115–125.

Mahony, R., Hamel, T., & Pflimlin, J. M. (2008). Nonlinear complementary filters on the special orthogonal group. *IEEE Transactions on Automatic Control*, *53*, 1203–1217.

Pathak, K., Franch, J., & Agrawal, S. K. (2005). Velocity and position control of a wheeled inverted pendulum by partial feedback linearization. *IEEE Transactions on Robotics*, *21*(3), 505–513.

Romlay, M. R., Ibrahim, A. M., Toha, S. F., & Rashid, M. (2019). Two-wheel balancing robot; review on control methods and experiments. *International Journal of Recent Technology and Engineering (IJRTE)*, *7*(6), 106–112.

Sun, W., Su, S. F., Xia, J. W., & Wu, Y. Q. (2020). Adaptive tracking control of wheeled inverted pendulums with periodic disturbances. *IEEE Transactions on Cybernetics*, *50*(5), 1867–1876.

Tian, J., Ding, J., Tai, Y. P., & Ma, Z. S. (2020). Control of different-axis two-wheeled self-balancing vehicles. *IEEE Access*, *8*.

Yan, X. G., Edwards, C., & Spurgeon, S. K. (2007). Output feedback sliding mode control for non-minimum phase systems with non-linear disturbances. *International Journal of Control*, *77*(15), 1353–1361.

Yan, X. G., Spurgeon, S. K., & Edwards, C. (2009). On discontinuous static output feedback control for linear systems with nonlinear disturbances. *Systems & Control Letters*, *58*(5), 314–319.

Yan, X. G., Spurgeon, S. K., & Edwards, C. (2017). *Variable Structure Control of Complex Systems*. Springer, Berlin, Germany.

Yue, M., An, C., & Li, Z. J. (2018). Constrained adaptive robust trajectory tracking for wip vehicles using model predictive control and extended state observer. *IEEE Transactions on Systems, Man, and Cybernetics: Systems*, *48*(5), 733–742.